

## WIDE-FIELD IMAGING WITH MOSAIC CCD CAMERAS

S. OKAMURA,<sup>1</sup> M. DOI,<sup>1</sup> W. KAWASAKI,<sup>1</sup> Y. KOMIYAMA,<sup>1</sup> K. SHIMASAKU,<sup>1</sup> M. YAGI,<sup>1</sup> N. YASUDA,<sup>1</sup> N. KASHIKAWA,<sup>2</sup>  
AND M. SEKIGUCHI<sup>2</sup>

<sup>1</sup>Department of Astronomy and Research Center for the Early Universe,  
School of Science, University of Tokyo, Bunkyo-ku, Tokyo, 113 Japan

<sup>2</sup>National Astronomical Observatory, Mitaka, Tokyo, 181 Japan

### ABSTRACT

An outline is given of our development of mosaic CCD cameras. Hardware and data reduction software of two operational cameras are described. Scientific objectives of wide-field imaging with the cameras are briefly described.

*Key Words* : mosaic CCD camera, imaging

### I. INTRODUCTION AND BACKGROUND

Around 1988, when we started the development of a mosaic CCD camera, CCDs available at a reasonable price were 1K chips that had a size of about 1 cm<sup>2</sup>. Schmidt photographic plates, on the other hand, had a size of about 1000 cm<sup>2</sup>. If we define the *survey efficiency* by  $(\text{sensitivity}) \times (\text{detector area})$ , even with a 100 times higher sensitivity, CCDs could not cope with photographic plates. The increase of the effective area of CCDs by mosaicking was of critical importance for wide-field surveys (e.g., Kron 1995).

There were two approaches to the CCD mosaicking. One was the 'as-close-as-possible' approach that was based on abutable CCDs. The other was the 'ample-gap' approach which used usual packaged CCDs. Most groups in the world followed the former approach, which is orthodox but technically more difficult because one has to deal with bare CCDs. We, on the other hand, decided to take the latter approach. This is why we could construct our first mosaic CCD camera (hereafter M CCD1) consisting of 2×8 array of 1K chips as early as 1991.

After we finished the development of M CCD1 (1988-1991), we constructed the second mosaic CCD camera (hereafter M CCD2; 1991-1995) consisting of 5×8 array of the same 1K chips as in M CCD1. Some of us have been involved in the development of the main imaging camera for the Sloan Digital Sky Survey (Gunn and Knapp 1993; Okamura 1995) in collaboration with the astronomers in the USA (1993-1996). These three cameras are based on the packaged CCDs. The last one we are constructing (1996-1998) is a wide-field prime focus camera for the 8.2m Subaru telescope (Iye et al. 1996), which will employ the 2×5 array of 2K×4K abutable CCDs.

We have also developed a set of data reduction programs dedicated to our mosaic CCD cameras. The origin of the software is the one developed for the automated surface photometry of faint galaxies using digitized photographic data (Doi et al. 1995). Efforts have been made continuously to enhance the function of the software.

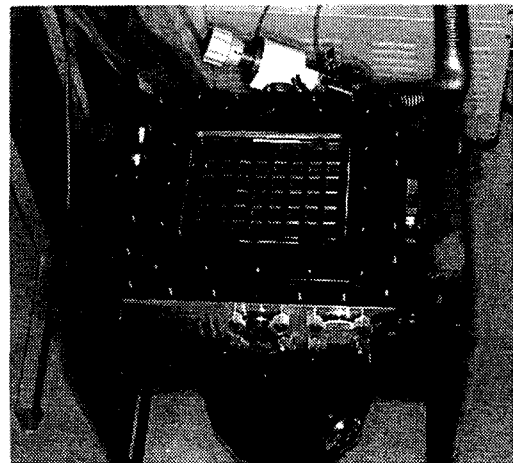


Fig. 1.— The mosaic CCD camera. Forty 1k×1k CCDs are mounted in the 5×8 array.

In this report we concentrate on hardware and software of M CCD1 and M CCD2 and scientific objectives of wide-field imaging observations with them.

### II. CAMERA HARDWARE

M CCD1 consisted of the 2×8 array of TC215 CCDs (1K×1K; 12μm pixel) manufactured by TI Japan. TC215 is a virtual phase CCD, which has a peak QE of 60% at 700 nm and 15% at 350 nm (Takato et al. 1990). TC215 is available commercially in a usual 24-pin package. M CCD1 was dedicated to the 105cm Kiso Schmidt telescope; the 16 CCD chips were mounted on the spherical surface to match the focal plane of the Schmidt telescope (Sekiguchi et al. 1992).

On the other hands, M CCD2 has been made for the flat focal plane so as to realize its portability (Kashikawa et al. 1995b). In fact, we made observations with M CCD2 at the Cassegrain focus of the 40-inch Swope telescope at Las Campanas in 1994-95, and at the prime focus of William Herschel Telescope (WHT) at La Palma in 1996. M CCD2 uses the same CCDs as in M CCD1 but in a specially de-

signed compact package. The gap between adjacent chips is smaller in M CCD2. The array size of M CCD2 evolved from the  $7 \times 4$  array in April 1994 to the  $8 \times 5$  array in April 1995. One contiguous field of M CCD2 ( $8 \times 5$  array) observation is composed of four (eight in some cases where one needs higher photometric accuracy) offset exposures. It consists of  $9,280 \times 14,500$  pixels, corresponding to  $0.^\circ 90 \times 1.^\circ 41$  ( $0.^\circ 35/\text{pixel}$ ) for the Swope telescope and  $0.^\circ 54 \times 0.^\circ 85$  ( $0.^\circ 21/\text{pixel}$ ) for WHT. We are not using M CCD1 any more because of the advent of M CCD2.

M CCD1 and 2 are based on the same technology except for the differences noted above. Each chip is mounted on a machined ceramic spacer whose thermal expansion coefficient is similar to that of the CCD package. The chip was glued on the spacer with two tungsten-copper wires in between the chip and the spacer. The glue was Ag-based conductive epoxy. The  $x$ - $y$  positions and the height  $z$  was monitored using a microscope while the chip was glued. The role of the wires are two-fold. One is to make the thickness of the glue constant and the other is to fine adjust the  $z$ -position with wires of different diameters to allow for chip-to-chip difference. The spacer with a chip glued on it was glued (M CCD1) or screwed (M CCD2) to the copper mother board with the help of an accurate gauge. The accuracy we achieved was  $30 \mu\text{m}$  in all  $x$ ,  $y$ , and  $z$  directions.

We use the VME-based control system called MESIA2 (Modularized Expandable System for Image Acquisition). Five columns of M CCD2, each consisting of 8 CCDs, are read in parallel while 8 CCDs in a column are read sequentially. It takes about 100 seconds to complete reading the 40 CCDs and storing the data in the VME memory. It is the dead time between the two exposures. The CCDs are cooled by liquid nitrogen down to  $-90^\circ\text{C}$ . The dewar of M CCD2 is  $30\text{cm} \times 30\text{cm} \times 10\text{cm}$  in size and weighs about 40 Kg including a tank for liquid nitrogen. M CCD2 as of April 1996 is shown in Figure 1.

Some performance characteristics of M CCD2 are summarized below. Average ADC conversion factor is  $2.8e/\text{ADU}$ , average read noise is  $7.8e$ , dark current is negligible at  $-90^\circ\text{C}$  for a 20 minutes exposure, linearity is better than 3% over 300–6000e. There are chip to chip variations in the ADC conversion factor (14%), read noise (10%), and bias level (13%), but they are all stable and causes little errors in excess of those found in the single chip operation.

A large two-board focal plane shutter was made. 'Open' and 'close' are effected by the sliding motions of the two boards in turn so that the exposure time is nearly uniform over the wide field of view. Large filters of  $24\text{cm} \times 24\text{cm}$  have been prepared for  $U$ ,  $B$ ,  $V$ ,  $R$ ,  $I$  and  $Z$  bands.

### III. DATA REDUCTION SOFTWARE

The data reduction software is developed by our group. It is written in *C* and driven by *esh* script to assure good portability. One contiguous field usually consists of  $\sim 1\text{GB}$  of raw data including calibration data such as bias, dark, and flat fields, and produces additional  $\sim 3\text{GB}$  of intermediate data such as sky-subtracted data. Because of this large amount of data to be processed, we have made the software as automated as possible. However, we also implemented in the software the functions to compute variety of image statistics and plot them for quick look at several stages of the processings. We can check with these plots whether the data are being processed properly. Our main interest lies in faint galaxies and quasars. The software is therefore optimized for surface photometry of such objects.

The data reduction proceeds as follows. Most processings are the same as those in case of a single-chip CCD camera. First, the raw data are cleaned, i.e., bias/dark is subtracted, cosmic rays are removed, and the geometric distortion is corrected, if necessary. The cleaned frames ( $8 \times 5 \times 4 = 160$  frames) are then flat-fielded. The flat field is made for each of the 40 chips using both the dome-flat/twilight and object frames taken during an observing run. The local sky background is defined for each of the 160 frames as follows. Each frame is divided into subframes consisting of  $N \times N$  pixels. Here  $N$  is a tunable parameter chosen so that  $N$  pixels roughly correspond to the largest size above which objects are not searched. The histogram of the  $N^2$  pixel values is made and the portion around its peak is fit by a Gaussian to yield the pixel value at the peak of the histogram. The pixel values at the peak are assigned to the center of the respective subframes and subjected to a median filtering to avoid the effect of very bright objects possibly located in a few subframes. The median-filtered values are finally interpolated to the original pixels bi-linearly to define the local sky background at the pixels (Fig.2). The local sky is subtracted from the frame.

Now we proceed to the pre-processings characteristic of our camera. In order to assure the uniformity of the object detection and photometric parameters, the image quality should be made as homogeneous as possible over a contiguous field. The FWHM of the PSF is measured for all the 160 frames from the four offset exposures. The largest PSF (worst seeing) is taken to be the target. The Gaussian smoothing is applied to the frames with smaller PSFs so that the resulting frames have the target PSF. We proceed to the frame mosaicking next in order to establish a consistent coordinate system and a consistent flux scale over a contiguous field composed of four separate offset exposures taken by 40 different chips. This is accomplished by comparing the positions and fluxes of the same objects which fall in the overlapped region and measured in different exposures/chips (cf. Fig.3). Aperture fluxes are

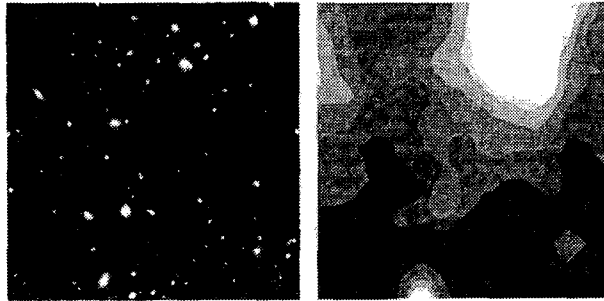


Fig. 2.— Cleaned and flat-fielded frame (left) and the local sky background for the frame.

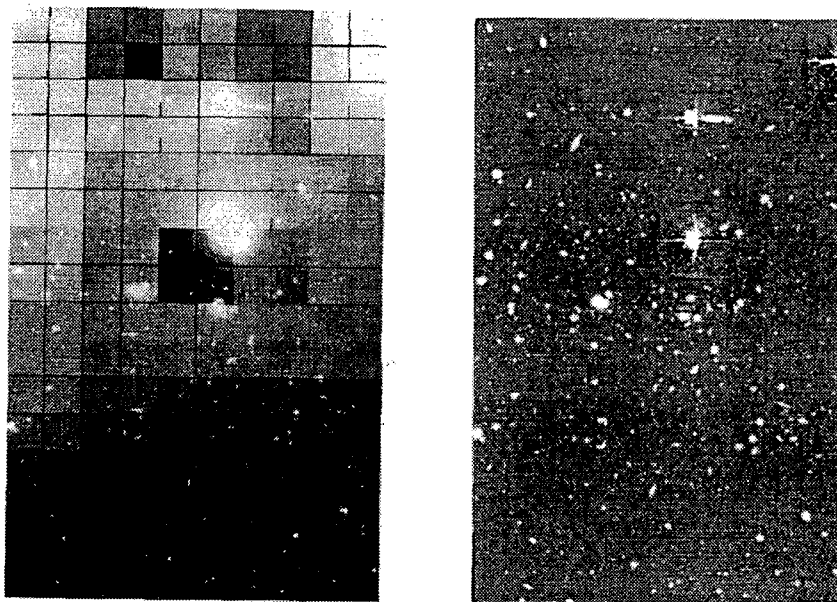


Fig. 3.— All the 160 frames before frame mosaicking (left) and the mosaicked image for a contiguous field (right).

used here because isophotal fluxes are affected by even a subtle difference in the image quality among frames. Twilight frames are also used to measure chip-to-chip sensitivity variation.

The R-band data of 20 minutes exposure for the Coma cluster were used to estimate the photometric and positional accuracies. The data were taken with MCCD1 at the F/3 prime focus of the 105-cm Kiso Schmidt and consisted of 15 offset exposures covering a large  $3.4 \times 1.65$  contiguous field. The internal accuracy of the photometry is estimated by the magnitude difference of the same stars in different exposures/chips after frame mosaicking. The rms error is 0.08 mag in  $17.5 < R < 18.0$  (Fig.4). The dominant components contributing to the error are photon noise and the small scale pattern seen in the bias frame. The positional accuracy is estimated using 260 stars in the Guide Star Catalog (Lasker et al. 1990) as position reference stars. The rms residuals are about 0."6 in right ascension and 0."5 in declination.

The mosaicked and PSF-equalized data of a contiguous field is subjected to the more or less usual image analysis consisting of object detection, measurement of photometric and shape parameters, and star/galaxy discrimination. We further classify galaxies into two crude classes, 'early-type' and 'late-type', on the basis of the luminosity concentration and the mean surface brightness (Doi et al. 1993). Early-types are galaxies with luminosity profiles resembling the  $r^{1/4}$ -law while late-types are those with profiles resembling the exponential law.

#### IV. SCIENTIFIC OBJECTIVES

We have two primary scientific objectives of observations with our mosaic CCD cameras.

One is to construct a multi-color photometric database of nearby ( $z \lesssim 0.2$ ) clusters of galaxies. In contrast to the rapid growth of modern photometry data of distant clusters with the use of CCD detectors at large telescopes (e.g., Dressler and Gunn 1992) and HST (e.g.,

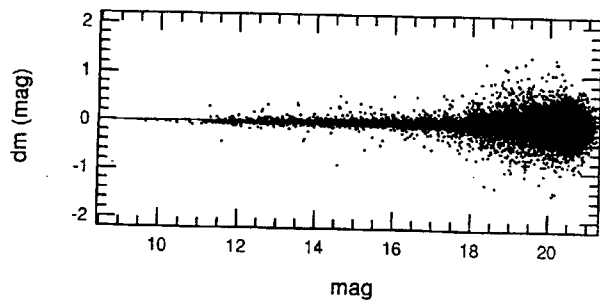


Fig. 4.— Internal photometric accuracy as a function of magnitude.

Dressler et al. 1994), there is little progress in the observations of clusters at low and intermediate redshifts ( $z \lesssim 0.2$ ). At present, the photometric data for clusters at  $z \lesssim 0.2$  mainly come from photographic photometry. It is very important to collect high-quality data, especially magnitudes, colors and morphology, of galaxies in clusters at  $z \lesssim 0.2$  using CCD detectors. The lack of CCD data for such clusters is simply due to the fact that no CCD camera had been available until recently that covers the wide extension of clusters within the reasonable amount of observing time. We want to use our MCCD2 to make a breakthrough in this field.

We observed more than a dozen of nearby ( $z \lesssim 0.2$ ) clusters of galaxies in the  $B$ ,  $V$ , and  $R$  bands with MCCD2 attached to the Swope telescope. We have been measuring positions, magnitudes, colors, and shapes of galaxies down to  $R \sim 20$  mag, and coarse morphological types down to  $R \sim 19$  mag for the clusters. The specific topics we want to address include type-specific luminosity function, dwarf population, color magnitude relation of early-type galaxies, morphology and luminosity segregation, and Butcher-Oemler effect. We want to investigate the dependence of such properties of galaxies on global properties of clusters and/or on galaxy density, and compare the results with those for more distant clusters. The initial result was published by Kashikawa et al. (1995a). Based on the  $R$ -band data of four clusters, A1656(Coma;  $z = 0.02$ ), A1367( $z = 0.02$ ), A1644( $z = 0.05$ ), and A1631( $z = 0.05$ ), they detected a significant cluster-to-cluster variation in the faint part ( $M_R \gtrsim -18$ mag) of the luminosity function of early-type galaxies.

The other objective is to survey general fields such as NGP and SGP. We aim to search for high-redshift quasars, obtain deep galaxy counts for wide fields and study angular correlation function of faint galaxies. The wide field of view of our MCCD2 is also useful to optical identification of sources found in the survey at various wavelengths.

## REFERENCES

- Doi, M., Fukugita, M., & Okamura, S. 1993, *MNRAS*, 264, 832.

Doi, M., Fukugita, M., & Okamura, S. 1995, *ApJS*, 97, 59.

Dressler, A., & Gunn, J.E. 1992, *ApJS*, 78, 1.

Dressler, A., Oemler, A.Jr., Sparles, W.B., & Lucas, R.A. 1994, *ApJ*, 435, L23.

Gunn, J.E., and Knapp, G.R. 1993, in *Sky Surveys: Protostars to Protogalaxies*, ASP Conf., Vol.43, ed. B.T.Soifer (Provo: Brigham Young Univ.), p.267.

Iye, M. et al. 1996, *SPIE*, 2871 (in press)

Kashikawa, N., Shimasaku, K., Yagi, M., Yasuda, N., Doi, M., Okamura, S., & Sekiguchi, M. 1995a, *ApJ*, 452, L99.

Kashikawa, N. et al. 1995b, in *Scientific and Engineering Frontiers for 8-10m Telescopes*, eds. M.Iye and T.Nishimura (Tokyo: Universal Academy Press), p.105.

Kron, R.G. 1995, *PASP*, 107, 766.

Lasker, B.M. et al. 1990, *AJ*, 99, 2019.

Okamura, S. 1995, in *Scientific and Engineering Frontiers for 8-10m Telescopes*, eds. M.Iye and T.Nishimura (Tokyo: Universal Academy Press), p.33.

Sekiguchi, M., Iwashita, H., Doi, M., Kashikawa, N., & Okamura, S. 1992, *PASP*, 104, 744.

Takato, N., Aoki, T., Ichikawa, S., & Iye, M. 1990, *SPIE*, 1235, 242.